Two-Dimensional Crystallization of Annexin A5 on Phospholipid Bilayers and Monolayers: A Solid−Solid Phase Transition between Crystal Forms

Ilya Reviakine,[†] Wilma Bergsma-Schutter,[†] Alexander N. Morozov,[†,‡] and Alain Brisson*,[†]

Department of Biophysical Chemistry, GBB, University of Groningen, Nijenborgh 4, 9747 AG Groningen, The Netherlands, and Soft Condensed Matter Group, LIC, Leiden University, P.O. Box 9502, 2300BA Leiden, The Netherlands

Annexin A5 is a soluble protein which binds to negatively charged phospholipids, such as dioleoylphosphatidylserine (DOPS), in the presence of Ca^{2+}. A solid−solid phase transition between two two-dimensional crystal forms of annexin A5, p6 and p3, previously identified by electron microscopy (EM), was studied in situ on supported phospholipid bilayers (SPBs) by atomic force microscopy (AFM) and ex situ on lipid monolayers by EM. The ability to directly vary the protein surface density on SPBs allowed a delicate and systematic way to investigate the reversibility of the transition with the AFM. The p6 crystal form was found to form first and to cover the entire lipid surface available, at all DOPS concentrations studied (5−95%). An increase in protein surface density, achievable only on SPBs (or monolayers) containing sufficient amounts of DOPS, destabilized the p6 phase. The transition to the more compact (p3) form occurred via local melting of the p6 phase at defects, such as grain boundaries, initially present in p6 crystals. On mono- or bilayers with lower DOPS contents, the density-dependent p6−p3 transition was not observed, but the p3 crystal form could still be reached by disturbing the system mechanically.

Introduction

Successful attempts to obtain protein crystals date back to 1840s.[1] Since that time, the procedures for obtaining them have remained largely empirical.[2] The complexity and the richness in the phase behavior exhibited by colloidal systems, compounded with the immensely complicated multicomponent mixtures typically used to obtain three-dimensional (3D) protein crystals, have contributed to the situation. Yet, behind this complexity lie the basic principles which govern the behavior of the constitutive species, and recent years have witnessed a tendency toward rationalization of macromolecular crystallization[2] exemplified by an increasing number of theoretical[3] and experimental[4−6] investigations into basic questions concerning the mechanism by which 3D protein crystals grow. The accent on these studies on 3D protein crystals is largely due to their usefulness in obtaining structural information using X-ray crystallography techniques.

Apart from the fact that two-dimensional (2D) protein crystals allow molecular structure determination at near-atomic resolution by electron crystallography,[7−9] understanding their formation may be relevant to that of 3D protein crystals. For instance, 2D nucleation has been identified as one of the mechanisms by which 3D protein crystals grow,[4] and 2D protein crystals have been found at the edges of 3D crystallization droplets[10] and have been implicated as intermediates in the formation of the 3D crystals in the case of several soluble proteins.[11,12] Furthermore, 2D systems are expected to exhibit behavior distinct from that of the 3D ones (cf. ref 13). Large, ordered 2D arrays of proteins on solid supports are also of potential interest for the field of nanotechnology.

A number of recent studies of 2D crystallization of proteins on lipid monolayers, the technique of choice for crystallizing soluble proteins in two dimensions,[14−16] have focused on the liquid−solid transition.[17−20] Solid−solid

---

(1) McPherson, A. *J. Cryst. Growth* **1991**, *110*, 1 and references therein.

(2) Giegé, R.; Ducruix, A. In *Crystallization of Nucleic Acids and Proteins: A practical Approach*; Ducruix, A., Giegé, R., Eds.; Oxford University Press: Oxford, 1999; p 1.

(3) ten Wolde, P. R.; Frenkel, D. *Science* **1997**, *277*, 1975.

(4) Malkin, A. J.; Kuznetsov, Yu. G.; Land, T. A.; DeYoreo, J. J.; McPherson, A. *Nat. Struct. Biol.* **1995**, *2*, 956.

(5) Kuznetsov, Yu. G.; Malkin, A. J.; McPherson, A. *J. Cryst. Growth* **1999**, *196*, 489.

(6) Kuznetsov, Yu. G.; Malkin, A. J.; McPherson, A. *Phys. Rev. B* **1998**, *58*, 6097.

(7) Henderson, R.; Baldwin, J. M.; Ceska, T. A.; Zemlin, F.; Beckmann, E.; Downing, K. H. *J. Mol. Biol.* **1990**, *213*, 899.

(8) Kimura, Y.; Vassylyev, D. G.; Miyazawa, A.; Kidera, A.; Matsushima, M.; Mitsuoka, K.; Murata, K.; Hirai, T.; Fujiyoshi, Y. *Nature* **1997**, *389*, 206.

(9) Nogales, E.; Wolf, S. G.; Downing, K. *Nature* **1998**, *391*, 199.

(10) Cyrklaff, M.; Auer, M.; Kühlbrandt, W.; Scarborough, G. A. *EMBO J.* **1995**, *14*, 1854.

(11) Hemming, S. A.; Bochkarev, A.; Darst, S. A.; Kornberg, R. D.; Ala, P.; Yang, D. S. C.; Edwards, A. M. *J. Mol. Biol.* **1995**, *246*, 308.

(12) Edwards, A. M.; Darst, S. A.; Hemming, S. A.; Li, Y.; Kornberg, R. D. *J. Struct. Biol.* **1994**, *1*, 195.

(13) Strandburg, K. J. *Rev. Mod. Phys.* **1998**, *60*, 161.

(14) Uzgiris, E. E.; Kornberg, R. D. *Nature* **1983**, *301*, 125.

(15) Brisson, A.; Olofsson, A.; Ringler, P.; Schmutz, M.; Stoylova, S. *Biol. Cell* **1994**, *80*, 221.

(16) Kubalek, E. W.; Kornberg, R. D.; Darst, S. A. *Ultramicroscopy* **1991**, *35*, 295.

(17) Frey, W.; Schif, W. R.; Vogel, V. *Langmuir* **1996**, *12*, 1312.

(18) Edwards, T. C.; Koppenol, S.; Frey, W.; Schief, W. R.; Vogel, V.; Stenkamp, R. E.; Stayton, P. S. *Langmuir* **1998**, *14*, 4683.

(19) Brisson, A.; Bergsma-Schutter, W.; Oling, F.; Lambert, O.; Reviakine, I. *J. Cryst. Growth* **1999**, *196*, 456.

(20) Vénien-Bryan, C.; Lenne, P.-F.; Zakri, C.; Renault, A.; Brisson, A.; Legrand, J.-F.; Berge, B. *Biophys. J.* **1998**, *74*, 2649.

(21) Wang, S.-W.; Robertson, C. R.; Gast, A. P. *Langmuir* **1999**, *15*, 1541.

(22) Yatcilla, M. T.; Robertson, C. R.; Gast, A. P. *Langmuir* **1998**, *14*, 497.

(23) Wang, S.-W.; Poglitsch, C. L.; Yatcilla, M. T.; Robertson, C. R.; Gast, A. P. *Langmuir* **1997**, *13*, 5794.
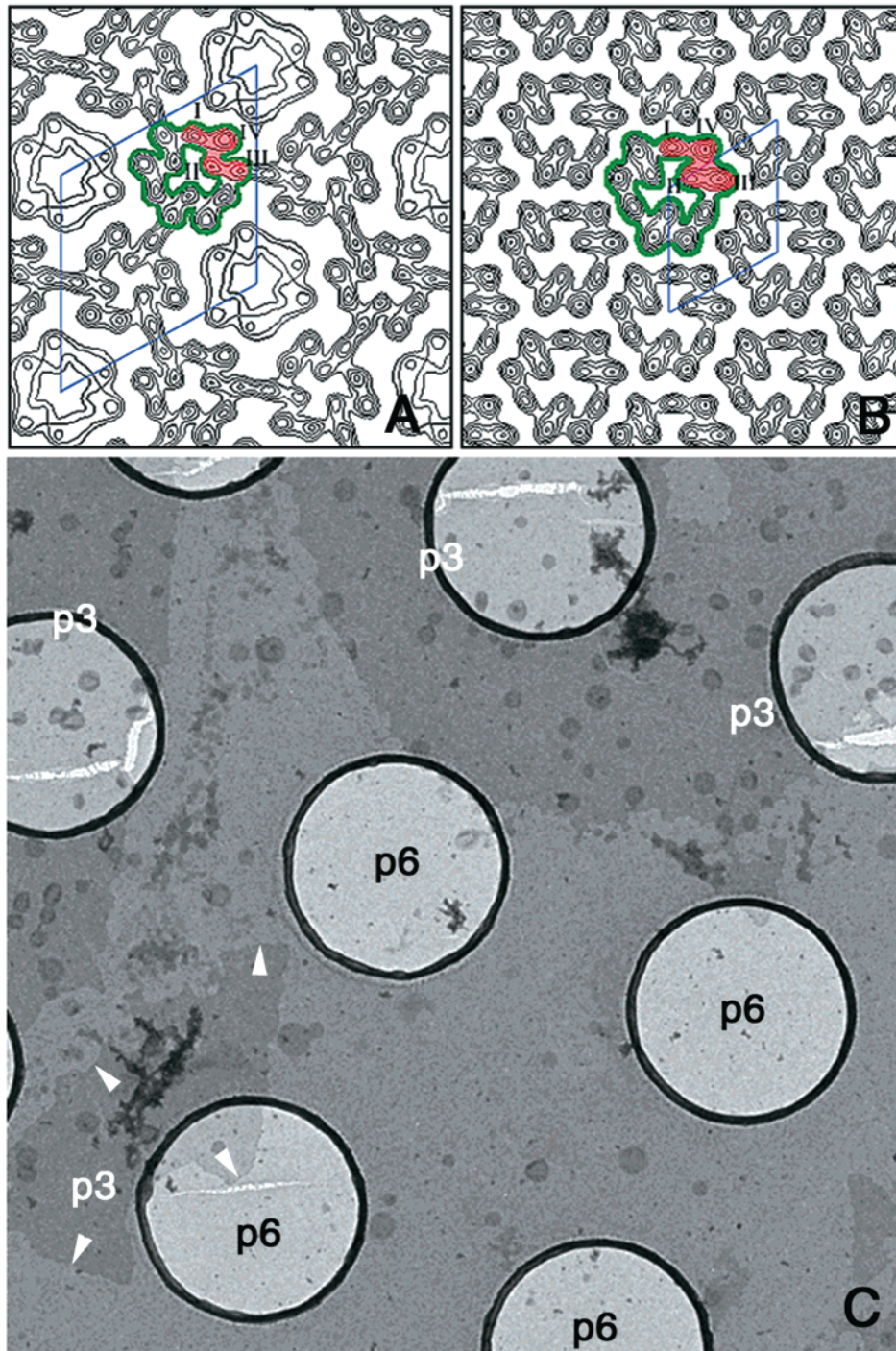
Figure 1. EM analysis of annexin A5 2D crystals grown at an air−water interface and transferred to EM grids. (A) 2D projection map of the p6 crystal form calculated from cryo-EM images at 2.0 nm resolution. The crystals were grown on lipid monolayers containing 20% DOPS and picked up with a perforated carbon film grid. Each trimer (one of which is outlined in green) is connected to three other trimers via the domains III of the individual annexin A5 monomers (red). Roman numerals (I−IV) refer to the individual domains making up the annexin A5 monomer (numbering after Huber et al. (ref 30)). The unit cell is $a = b = 17.7$ nm, $\gamma = 120°$. (B) 2D projection map of the p3 crystal form calculated from a cryo-EM image at 2.4 nm resolution. The crystals were grown in conditions identical to those described in (A) but picked up with a continuous carbon film grid. In this crystal form, each trimer (outlined in green) is connected to six other trimers. The unit cell is $a = b = 9.4$ nm, $\gamma = 120°$. (C) Annexin A5 crystals grown at the air−water interface were picked up with half-and-half grids. The p6 crystal form was found exclusively over the holes, whereas domains of the p3 crystal form were found on the intervening carbon film and frequently extended over the holes. One of the p3 domains is outlined with white arrowheads. The holes are 2 μm in diameter.

phase transitions between various crystal forms have so far been reported only for the streptavidin system.[21−23] The long-standing observation that two 2D crystal forms of annexin A5[24] exist, p6 (Figure 1A)[25] and p3 (Figure 1B),[19,26,27] has prompted this investigation of the relationship between them.

Annexin A5 is a 35 kD soluble protein which exists as a monomer in solution but forms trimers and 2D crystals upon binding, in the presence of Ca^{2+}, to phospholipid assemblies (monolayers, vesicles, or supported phospholipid bilayers (SPBs)) containing negatively charged phospholipids, such as dioleoylphosphatidylserine

(DOPS).[29] The structure of its soluble form has been solved by X-ray crystallography,[30] and that of the membrane-bound form was investigated extensively by electron crystallography[19,25–28] and, more recently, by atomic force microscopy (AFM).[31,32] The p6 crystal form of annexin A5 (Figure 1A) was observed when crystals grown on lipid monolayers were picked up with perforated carbon film grids.[19,25] The p3 crystal form was, until now, observed only after transfer to continuous carbon film grids[19,27] (Figure 1B), suggesting that the p6 form pre-exists at the air–water interface whereas transfer to a continuous carbon film results in formation of the p3 form.[19] The initial AFM observations of the p6 crystals formed on SPBs[31] lent strong support to this hypothesis. Both crystal forms have annexin A5 trimers as their basic building blocks (Figure 1A,B), as do most of the 3D annexin A5 crystal forms.[33] The two crystal forms have different protein densities (p3 is 1.2 times more dense than p6). The details of the surface topography of the two crystal forms have been discussed in refs 31 and 32, whereas this study addresses the issues of thermodynamic stability of the crystal forms and the mechanism of the transformation between them.

This study provides another example of the unique ability of AFM to reveal the dynamics of complex molecular processes.[34]

Materials and Methods

Materials. The lipids used in this study, DOPS, dioleoyl phosphatidylcholine (DOPC), and dipalmitoyl phosphatidylcholine (DPPC), were purchased from Avanti Polar Lipids (Alabama). Other chemicals were purchased from Merck (Germany) or Sigma (Missouri). Water used in this study was purified with a MilliQ water purification system (Millipore). All glassware was stored overnight in a mixture of chromic and sulfuric acids and rinsed thoroughly with water prior to use.

The buffers were as follows: (A) 2 mM $CaCl_2$, 150 mM NaCl, 10 mM HEPES, 3 mM NaN_3, pH 7.4; (B) 2 mM EDTA, 150 mM NaCl, 10 mM HEPES, 3mM NaN_3, pH 7.4; (C) 150 mM NaCl, 10 mM HEPES, 3 mM NaN_3, pH 7.4. All buffers were prepared in MilliQ water and filtered through a 200 nm syringe filter (Schleicher and Schuell, Germany) prior to use.

Recombinant rat annexin A5 was prepared as previously described.[32]

Electron Microscopy and Image Analysis of Annexin A5 2D Crystals Grown on Lipid Monolayers. 2D crystals of annexin A5 were grown on lipid monolayers at an air–water interface as described in detail in ref 35. Briefly, lipid monolayers were prepared by applying 0.6 μL of a given mixture of DOPC

and DOPS dissolved in chloroform/hexane (1:1, v/v) over a 17 μL droplet of 0.1 mg/mL annexin A5 in buffer A. Two types of supports were used to pick up the material present at the air–water interface after an overnight incubation: electron microscopy (EM) grids coated with a perforated carbon film (so-called "holey" grids, prepared by method a in ref 35) or grids exhibiting a regular array of 2 μm diameter holes in the carbon support (Quantifoil Micro Tools GmbH, Jena, Germany).[36] In the latter case, the holes covered ~50% of the total surface area; hence, these grids will be referred to as "half-and-half" grids.

The grids were stained with 1% uranyl acetate, coated with a thin layer of carbon to increase their stability, and observed in a Philips CM120 transmission electron microscope operated at 120 kV. Images were recorded with a 1k×1k Gatan CCD camera. The p6 and p3 domains were identified from the characteristic appearance of their respective Fourier transforms.[19]

Atomic Force Microscopy. Continuous SPBs containing 20–95% DOPS were prepared by depositing 100 μL of sonicated vesicle suspension containing ~0.5 mg/mL of the appropriate lipid mixture in buffer A on a freshly cleaved mica disk and incubating for 30–60 min at about 20 °C. The process of SPB formation can be controlled by adjusting the lipid concentration and incubation time.[37] In particular, incubating a ~0.06 mg/mL vesicle suspension for ~1 h resulted in an incomplete SPB made of isolated single bilayer disks (used in reversibility experiments). Excess vesicles were removed by repeated washing with buffer A. SPBs containing ~80% DOPS exhibited a tendency toward multilayer formation and required washing with buffer B for a clean, single SPB to be obtained. More extensive details concerning SPB formation can be found in ref 37.

A few (3–30) microliters of a concentrated (0.6 mg/mL) annexin A5 solution was added to the 100 μL of subphase above the SPB for the AFM experiments. Consequently, the Ca^{2+} concentration varied between 1.5 and 2 mM.

Preparation of AFM samples has been described in detail in refs 31, 32, and 37 and relied on the procedure due to Müller et al.[38] Images were acquired in buffer, in constant force mode using a Nanoscope IIIa-MultiMode AFM (Digital Instruments, CA) equipped with a J (120 μm) or an E (16 μm) scanner and oxide sharpened silicon nitride tips mounted on cantilevers with a nominal force constant of 0.06 N/m, at scanning rates of 8–15 Hz and a scan angle of 90° at the lowest possible imaging force. The contact mode fluid cell (Digital Instruments) was washed extensively with 95% ethanol and water before each experiment. O-rings, washed in 1% Helmanex solution (GMBH, Germany) overnight and sonicated 3× in freshwater, were used in experiments where exchange of buffers was required.

Results

Electron Microscopy. To complement the existing information concerning the effect a transfer to EM grids has on the observed crystal form of annexin A5,[19] the crystals grown on lipid monolayers containing 20% DOPS at the air–water interface were picked up with half-and-half grids (Figure 1C). Consistent with the previous findings, the p6 crystal form was found only over holes, whereas the p3 form was found on the continuous carbon film regions of the half-and-half grids. The p3 domains were often found to extend over the holes (Figure 1C). A clear difference in grayness was observed between the two forms, which may mean a different height, different mass density, or different staining characteristics. Because films transferred with perforated carbon film grids show only p6 crystals and no p3 domains,[19,25] the experiments with half-and-half grids directly implicate the transfer to the continuous carbon film as the cause of the transition.

(24) Annexin A5 is the new name for annexin V, according to the recently suggested nomenclature (see: Morgan et al. *Genomics* **1999**, *60*, 40.).

(25) Voges, D.; Berendes, R.; Burger, A.; Demange, P.; Baumeister, W.; Huber, R. *J. Mol. Biol.* **1994**, *238*, 199.

(26) Brisson, A.; Mosser, G.; Huber, R. *J. Mol. Biol.* **1991**, *220*, 199.

(27) Mosser, G.; Ravanat, C.; Freyssinet, J.-M.; Brisson, A. *J. Mol. Biol.* **1991**, *217*, 241.

(28) Oling, F.; Sopkova-De Oliveira Santos, J.; Govorukhina, N.; Mazères-Dubut, C.; Bergsma-Schutter, W.; Oostergetel, G.; Keegstra, W.; Lambert, O.; Lewit-Bentley, A.; Brisson, A. *J. Mol. Biol.* **2000**, *304*, 561.

(29) *Annexins: Molecular Structure to Cellular Function*; Seaton, B. A., Ed.; Chapman and Hall: New York, 1996.

(30) Huber, R.; Römisch, J. M.; Paques, E. P. *EMBO J.* **1990**, *9*, 3867.

(31) Reviakine, I.; Bergsma-Schutter, W.; Brisson, A. *J. Struct. Biol.* **1998**, *121*, 356.

(32) Reviakine, I.; Bergsma-Schutter, W.; Mazères-Dubut, C.; Govorukhina, N.; Brisson, A. *J. Struct. Biol.* **2000**, *131*, 234.

(33) Brisson, A.; Lewit-Bentley, A. In *Annexins: Molecular Structure to Cellular Function*; Seaton, B. A., Ed.; Chapman and Hall: New York, 1996; p 43.

(34) Engel, A.; Müller, D. *Nat. Struct. Biol.* **2000**, *7*, 715.

(35) Brisson, A.; Lambert, O.; Bergsma-Schutter, W. In *Crystallization of Nucleic Acids and Proteins: A practical Approach*; Ducruix, A., Giegé, R., Eds.; Oxford University Press: Oxford, 1999, p 341.

(36) Ermantraut, E.; Wohlfart, K.; Tichelaar, W. *Ultramicroscopy* **1998**, *74*, 75.

(37) Reviakine, I.; Brisson, A. *Langmuir* **2000**, *16*, 1806.

(38) Müller, D. J.; Amrein, M.; Engel, A. *J. Struct. Biol.* **1997**, *119*, 172.

Table 1. Type of Annexin A5 2D Crystal Obtained on Lipid Monolayers (EM) and SPBs (AFM) at Various Amounts of DOPS

% DOPS (by weight)	EM, perforated carbon film	AFM
20	p6	p6
40	a	p6 or p3
50	p3	p3
60	a	p3
75	"close-packed" trimers[b]	
80	a	p3
95	a	p3

[a] Not studied. [b] The polycrystallinity observed in the case of the p3 crystal form may be responsible for the apparent discrepancy between the EM and AFM observations of p3 crystals on the lipid mono- and bilayers with high DOPS contents, because a large number of small, randomly oriented crystalline domains clearly visible by AFM will be averaged over when analyzed by EM.

The lipid composition was found to have an effect on the crystal form in which annexin A5 crystallized. Using perforated carbon films, the p6 crystal form was observed on lipid monolayers containing 5−20% DOPS, whereas the p3 form was observed on monolayers containing 50% DOPS or more. On monolayers containing ∼75% DOPS, close-packed trimers were found instead of 2D crystals (Table 1).

Atomic Force Microscopy. The p6 and p3 crystal forms can be readily distinguished on AFM images because of the difference in lattice spacing (a wider lattice in the p6 (turquoise lines in Figures 2 and 3) vs a denser packing of the p3 form (Figure 2B,D)), domain size (p6 domains are large, micrometers in size,[31] whereas p3 domains are significantly smaller (Figure 2C)[32]), and the presence of point defects in the p6 form[31] (circles in Figures 2A and 3D).

The p6 crystal form was the only one observed on SPBs containing less than 40% DOPS. Attenuating the kinetics of growth of the p6 domains[31] by reducing the bulk protein concentration enabled the early stages of the p6−p3 transition, which occurred on SPBs containing 40% DOPS[39] or more (Figure 2), to be visualized. The growth of the p3 form was frequently observed to initiate at grain boundaries between the p6 domains (Figure 2D). At particularly low protein concentrations, addition of annexin A5 to the fluid cell was required to initiate the transition (Figure 2B); this is certainly due to the transport-limited regime existing in the unstirred AFM fluid cell. However, in all cases the onset of the transition corresponded to a complete coverage of the surface with p6 domains.

To ascertain whether p6 and p3 crystal forms represent thermodynamically stable states, the reversibility of the p6−p3 transition was investigated with AFM. Two methods were used to directly vary the surface density of annexin A5 on an SPB. The first method (Figure 3) exploited the dependence of annexin A5 binding to phospholipid bilayers on the presence of Ca^{2+}. Crystals (p3 or p6 form) grown on an SPB were washed with a Ca^{2+}-free buffer. This resulted in a slow dissolution of the crystals because of a displacement of annexin A5 molecules from the SPB surface to the subphase. Flushing the cell and reintroducing a Ca^{2+}-containing buffer allowed the system to equilibrate at a new, lower surface density. Subjecting p3 crystals to such a procedure invariably led to the p6 crystal form being observed (Figure 3A−D). If

this procedure was continued, the p6 crystals were found to dissolve completely (not shown).

The second method (results not shown) involved arresting the formation of an SPB prior to completion, at a stage where isolated single bilayer disks[37] were present on the mica surface. Crystals of suitable crystal form, p3 or p6, were prepared on the disks by adding an excess of annexin A5. After washing the excess of unbound annexin, fresh vesicles were added to the specimen. As the newly introduced vesicles proceeded to cover the mica surface and to coalesce with the crystal-covered single bilayer disks,[37] the lipid surface available to crystalline annexin A5 increased, resulting in a decrease in protein surface density. The p6 crystals could be dissolved completely using this procedure. When starting with the p3 crystal form, the p6 one invariably appeared on the disks. Experiments were performed to investigate whether the PS-content of the newly added vesicles had an influence on the process; a transition from p3 to p6 crystals was observed in each case.

Discussion

Relationship between the p6 and p3 Crystal Forms of Annexin A5: A 2D Solid−Solid Phase Transition. Historically, the p3 2D crystal form of annexin A5 was observed by EM first, when crystals were transferred with the so-called continuous carbon films.[26,27] The p6 crystal form was observed later on perforated carbon films.[25] The relationship between the two crystal forms has only recently begun to emerge.[19] Although the transfer of the interfacial film to a continuous carbon film support is analogous to the well-known Langmuir−Schaefer transfer, that with a perforated carbon film is more akin to picking up a film of soap with a loop. Consequently, the latter mode of transfer is more likely to reflect the true organization of the film at the air−water interface prior to the transfer step than the former. The observations made by EM on perforated carbon films correlate with the ones made by AFM on SPBs (Table 1). Furthermore, in situ AFM experiments provide direct evidence for the existence of both crystal forms within the same plane (Figures 2 and 3), and the experiments with half-and-half grids (Figure 1) implicate the stress associated with the transfer to continuous carbon film in the transition.

Investigating the growth of 2D crystals in situ with the AFM allows a delicate and systematic way to study the relationship between the crystal forms, because the poorly controlled transfer step (which nevertheless does lead to extremely reproducible results with respect to the crystal form observed) becomes unnecessary. In particular, the reversibility of the transition between the two crystal forms, a question not addressable by EM, could be investigated directly. The transition was shown to be reversible (Figures 2 and 3), indicating that both p6 and p3 represent thermodynamically stable phases. The coexistence of the two crystal forms (Figures 2 and 3) and the shattering of large p6 domains into many small p3 ones are both indicative of a first-order transition between the two. The streptavidin system presents the only other example of a protein system reported to date to exhibit 2D solid−solid phase transitions.[21−23]

Mechanism of the p6−p3 Transition. Having proven that the two 2D crystal forms of annexin A5 are in fact two thermodynamically stable phases and that a direct phase transition occurs between them, we can turn to the mechanism of this transition. In general, the interplay between the entropic and potential energy contributions to the free energy (which in this case is investigated as
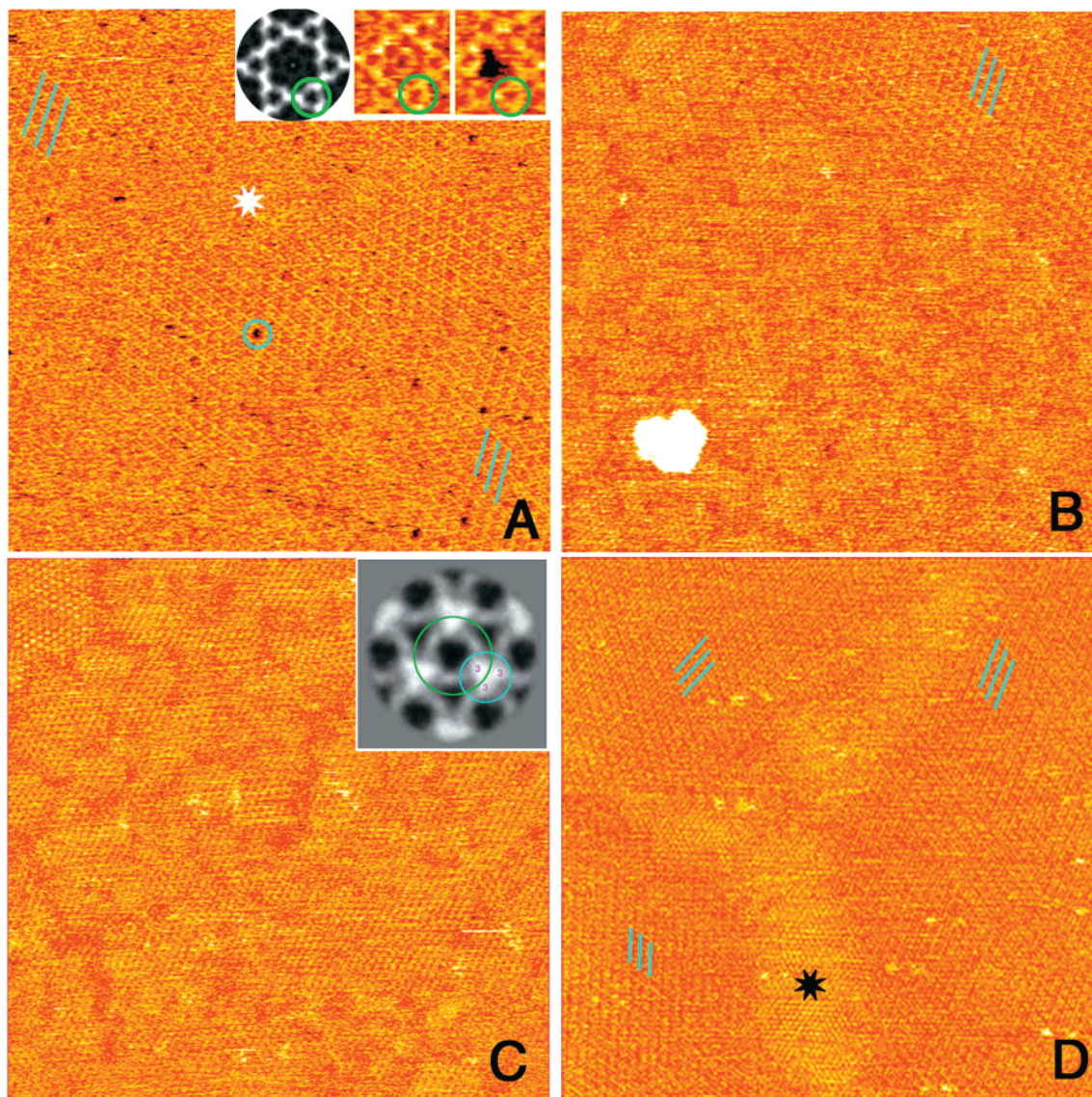
Figure 2. Forward p6–p3 transition, imaged by AFM. (A) The p6 crystal form on an SPB containing 80% DOPS. The lattice orientations of two p6 domains are indicated with turquoise lines. The p6 domains are separated by amorphous material (white asterisk). A number of vacancies (absences of the noncrystallographic trimer located at the 6-fold symmetry center of the lattice) are present. One such vacancy is encircled in turquoise and is shown in the left inset, alongside a regular arrangement of the trimers and an average topography map of the p6 crystal form calculated at 1.5 nm resolution (ref 32). Annexin A5 trimers are readily visible in the average topography map (encircled in green) as well as in the nonaveraged images (cf. Figure 1A). Image size (z-scale): 750 (3) nm. (B) Sample shown in (A), after addition of an excess of annexin A5. Most of the surface is covered with the p3 crystal form, but the p6 crystal form is still visible at the upper right corner. Scan size (z-scale): 720 (2.5) nm. (C) The transition to the p3 form proceeds to completion in the presence of excess annexin A5. Note the multiple small domains of the p3 form separated by wide grain boundaries. Scan size (z-scale): 600 (2.5) nm. Inset: Average topography map of the p3 crystal form (cf. Figure 1B) (ref 32). One of the annexin A5 trimers is encircled in green. (D) A p3 crystal domain (black asterisk) in the initial stage of growth at a grain boundary between three p6 domains (lattice orientations are indicated with turquoise lines) on an SPB containing 60% DOPS. Scan size (z-scale): 1200 (3) nm.

a function of protein surface density at a constant temperature) dictates which of the possible phases is observed (in this case, at a given value of protein surface density). Because two ordered phases are observed, the effective trimer–trimer interaction potential possesses at least two minima, corresponding to the two types of connectivity (Figure 1) and associated with specific interactions between the domains III in the case of p6 (Figure 1A) and a multiple set of interfacial interactions resulting from the tight packing between adjacent trimers in the case of p3 (Figure 1B). The shape of this potential remains unaffected by the changes in surface density which drive the transition observed on SPBs or by the mechanical stress associated with the transfer of the crystals to continuous carbon film grids.

Entropic considerations dictate that the less compact state (p6) occurs at a lower surface density, explaining the observation of the p6 form on SPBs of all compositions investigated (5–95% DOPS). The more compact, less symmetrical p3 phase can be reached only on SPBs (or monolayers) containing sufficient amounts of DOPS, namely, more than 40% DOPS[40] (from now on referred to as the critical DOPS concentration). Hence, at constant

(40) Mechanical stress associated with transfer of the crystals to continuous carbon film is sufficient to induce the p6–p3 transition on lipid monolayers containing 20% DOPS. It may be that the p3 phase observed by EM in these conditions is in a region of the phase diagram where it is metastable. This might explain why better ordered p3 crystals are usually observed in negatively stained preparations, which require drying, as compared to those embedded in vitreous ice, which do not.
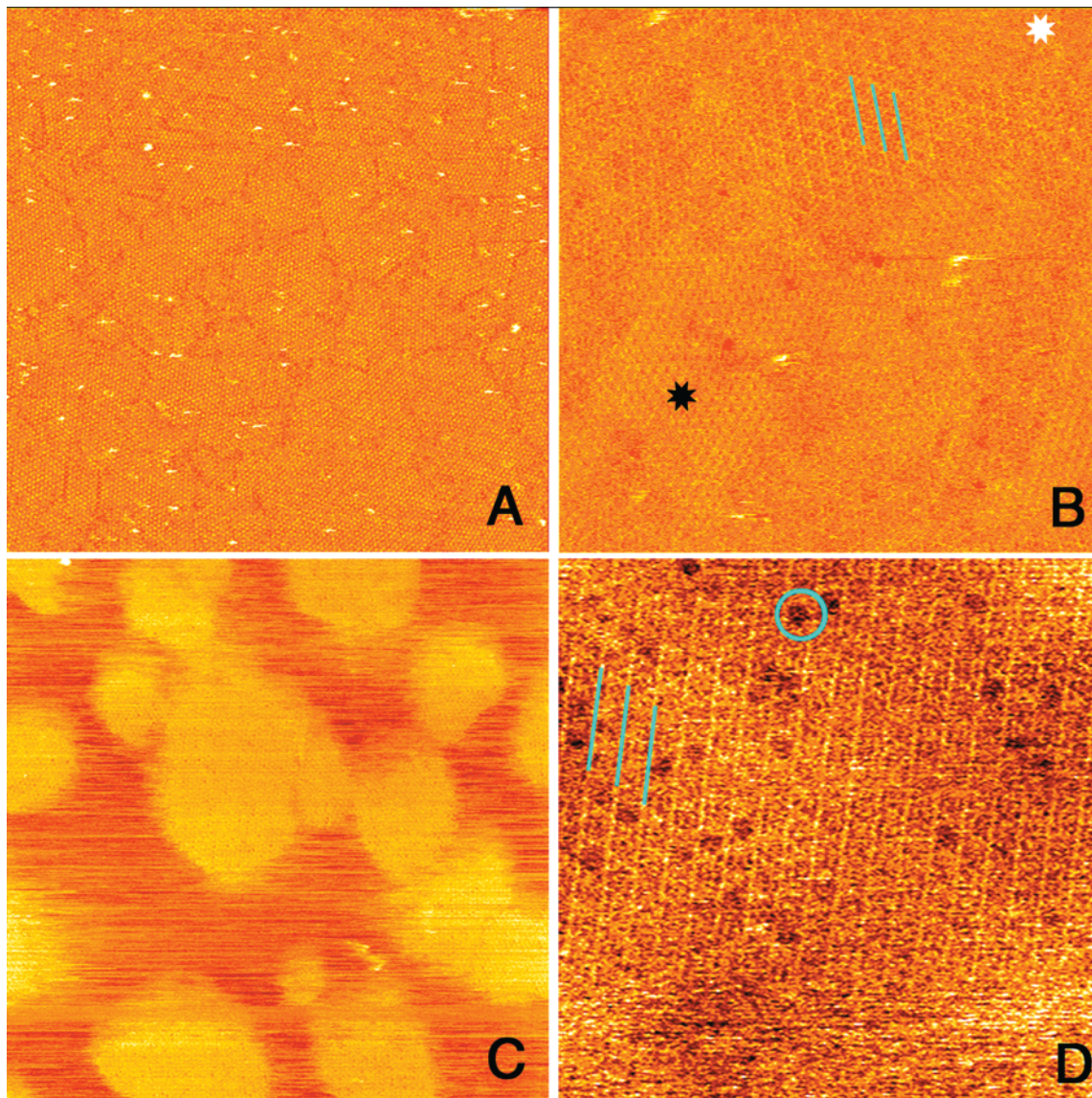
Figure 3. Reversibility of the p6−p3 transition. (A) A p3 crystal formed on a bilayer composed of 40% DOPS. Scan size (*z*-scale): 1.5 μm (5 nm). (B) Incubating the specimen shown in (A) in buffer C and washing with buffer A decreases the protein surface density (see text for discussion). This results in the appearance of the p6 crystal form (the lattice direction of one of the p6 domains is indicated with turquoise lines). The p3 crystal form is still visible on this image (black asterisk). Some amorphous material is visible as well (white asterisk). Scan size (*z*-scale): 580 nm (3 nm). (C) The p3 crystal form disappears completely after several incubations with buffer C followed by washes with buffer A. Only domains of the p6 crystal form (see (D)) are left. Scan size (*z*-scale): 2.6 μm (8 nm). (D) A high-magnification image of one of the domains shown in (C), clearly showing the p6 crystal form. One of the vacancies characteristic of the p6 domains is encircled in turquoise. Scan size (*z*-scale): 400 (5) nm.

Ca^{2+} concentration the DOPS content of the bilayer or monolayer controls the maximum attainable protein surface density. Because the same number of molecules in the p6 phase occupies a ~20% larger area than in the p3 one, the p3 nuclei, which will form spontaneously because of thermal fluctuations at the existing defects in the p6 lattice (such as grain boundaries, Figure 2D, and stacking faults[31]), will not be stable unless more annexin A5 monomers can adsorb from solution. This situation occurs only above the critical DOPS concentration. Multiple p3 domains which arise in this fashion will grow, creating numerous intersecting grain boundaries. The large domains of the p6 crystal form are hence shattered, and many small domains of the p3 one appear (Figures 2C and 3A).

The fate of the adsorbing monomers is not clear; they may either trimerize and join the growing p3 domains or remain as monomers occupying the wide grain boundaries observed in the p3 phase (Figures 2C and 3A; see also ref 32).

Comparison with Other Systems. The phenomena described here have relevance to other proteins crystallized on lipid monolayers.[19] In addition to the streptavidin system already mentioned, two crystal forms, p1 and p2, were found in the case of cholera toxin.[41,42] Some proteins, such as human factor Va, do not show crystals on perforated carbon films at all,[19] forming quasi-close-packed assemblies, but crystal formation can be induced by the transfer to continuous carbon films.[43]

(41) Ribi, H. O.; Ludwig, D. S.; Merger, K. L.; Schoolnik, G. K.; Kornberg, R. D. *Science* **1988**, *239*, 1272.
(42) Mosser, G.; Brisson, A. *J. Electron Microsc. Tech.* **1991**, *18*, 387.
(43) Stoylova, S.; Mann, K. G.; Brisson, A. *FEBS Lett.* **1994**, *351*, 330.

Conclusions

We have demonstrated that a solid−solid phase transition between the two 2D crystal forms, p6 and p3, of annexin A5 occurs on lipid monolayers and supported bilayers as a function of protein surface density and proposed a mechanism for the transformation.

Recent findings (to be published elsewhere) have implicated the p6 crystal form of annexin A5 in the inhibition of blood coagulation. On the basis of the fact that the transition from the p6 to the p3 form can be stress-induced, it is possible to speculate that the p3 form, too, has physiological relevance. Its formation in vivo may perhaps be associated with stresses resulting from changes in membrane curvature common to membrane-trafficking processes annexins are associated with.

LA001342L